Mesoscopic Kondo screening effect in a single-electron transistor embedded in a metallic ring

Hui Hu[1], Guang-Ming Zhang[1,2], Lu Yu[3,4]
[1] *Department of Physics, Tsinghua University, Beijing 100084, China*
[2] *Center for Advanced Study, Tsinghua University, Beijing 100084, China*
[3] *Abdus Salam International Center for Theoretical Physics, P. O. Box 586, Trieste 34100, Italy*
[4] *Institute of Theoretical Physics, Academic Sinica, Beijing 100080, China*
(February 1, 2008)

We study the Kondo screening effect generated by a single-electron transistor or quantum dot embedded in a small metallic ring. When the ring circumference L becomes comparable to the fundamental length scale $\xi_K^0 = \hbar v_F/T_K^0$ associated with the *bulk* Kondo temperature, the Kondo resonance is strongly affected, depending on the total number of electrons (*modulo* 4) and magnetic flux threading the ring. The resulting Kondo-assisted persistent currents are also calculated in both Kondo and mixed valence regimes, and the maximum values are found in the crossover region.

PACS numbers:72.15.Qm, 73.23.Ra, 73.23. Hk

The effect of magnetic impurities on metals— the Kondo problem has been studied for nearly half a century[1], and attracts continued interest till now in attempts to understand heavy fermion materials and high-T_c superconductors. Recent progress in the nanofabrication technique of electronic devices has enabled investigation of the Kondo effect by means of single-electron transistors (SETs) or quantum dots (QDs) in a controllable way[2–7]. When it contains an odd number of localized electrons, a QD may be described by the Anderson impurity model, exhibiting the Kondo effect characterized by the appearance of a sharp resonance near the Fermi energy[8,9], and it provides a new channel for electric current flowing through the QD.

To investigate the quantum phase interference, a device setup of a QD embedded in a mesoscopic metallic ring has been proposed[10–14]. In such a geometry the screening cloud is trapped in the ring, and one can measure the persistent current (PC) in the ring induced by the external magnetic flux to understand the coherent transport through the dot without attaching leads to it. Based on perturbation calculations, Affleck and Simon[14] recently pointed out that in the Kondo regime, the PC is a universal scaling function of ξ_K^0/L, where $\xi_K^0 = \hbar v_F/T_K^0$ is the characteristic length scale associated with the *bulk* Kondo temperature T_K^0, and crosses over from the value for a perfect ring with no QD in the limit $\xi_K^0/L \ll 1$ to a vanishing small magnitude for $\xi_K^0/L \gg 1$, in contrast to the variational calculations[13].

In this Letter, we would like to further clarify the underlying physics within a model of an Anderson magnetic impurity embedded in a mesoscopic metallic ring. Explicitly considering the discrete spectrum of conduction electrons in the ring using the slave boson mean field (SBMF) approach, we show that the Kondo resonance is strongly dependent on the ratio of ring circumference L to the screening cloud size ξ_K^0 ($L = N$, as the lattice spacing is assumed to be unity), the total number of electrons (*modulo* 4), and the magnetic flux threading the ring. The resulting Kondo-assisted PCs are calculated in both Kondo and mixed-valence regimes. Our numerical results are in good agreement with those of perturbation calculations in the limits of $\xi_K^0/L \ll 1$ and $\xi_K^0/L \gg 1$[14]. The *mesoscopic* Kondo effect was also studied in ultrasmall metallic grains[15].

SBMF approach. — A QD embedded in a mesoscopic Aharonov-Bohm (AB) ring can be described by a one-dimensional tight-binding Hamiltonian with N lattice sites including an Anderson impurity at site "0". The model Hamiltonian is given by:

$$H = -t\sum_{j=1}^{N-2}\sum_{\sigma}\left(c_{j\sigma}^{\dagger}c_{j+1\sigma} + h.c.\right) + Ud_{\uparrow}^{\dagger}d_{\uparrow}d_{\downarrow}^{\dagger}d_{\downarrow} + \sum_{\sigma}\left[\varepsilon_d d_{\sigma}^{\dagger}d_{\sigma} - \left(t_L d_{\sigma}^{\dagger}c_{1\sigma} + t_R e^{i\phi}c_{N-1\sigma}^{\dagger}d_{\sigma} + h.c.\right)\right]. \quad (1)$$

Here t_L (t_R) denotes the hopping between the QD and the left (right) neighboring site of the ring. The phase factor ϕ is defined by $2\pi\Phi/\Phi_0$, where Φ and $\Phi_0 = h/e$ are external magnetic flux and the flux quantum, respectively. We only consider a single spin-degenerate energy level ε_d of the QD. Since the Coulomb repulsion U is generally large in experiments, the limit of $U \to \infty$ can be taken. A parameter describing the coupling strength between the QD and the ring is introduced $\Gamma = \pi\rho(\varepsilon_F)\left|t(\varepsilon_F)\right|^2$, where $\rho(\varepsilon_F)$ and $t(\varepsilon_F)$ represent the ring density of states (DOS) and hopping at the Fermi energy ε_F, respectively. In this paper, only the half-filled case ($N_e = N$, where N_e is the total number of localized and delocalized electrons) is considered. In the thermodynamic limit, we would have $\varepsilon_F = 0$, $\rho(0) = N/(2\pi t)$, $t^2(0) = 2(t_L^2 + t_R^2)/N$, and $\Gamma = (t_L^2 + t_R^2)/t$.

The strong coupling SBMF theory has been well-known to be a good approximation in describing the Kondo physics at low temperatures. Here we will apply this method to the Anderson impurity model in the presence of a magnetic flux, and we believe that it can

still yield reliable results. Because of the infinite U limit, the impurity operator can be expressed as $d_\sigma^\dagger = f_\sigma^\dagger b$ in the slave-boson representation, where the fermion f_σ and the boson b describe the singly occupied electron and hole states, respectively. The constraint $b^\dagger b + \sum_\sigma f_\sigma^\dagger f_\sigma = 1$ has to be imposed. When the mean field (MF) approximation is made, the boson operators are replaced by a c-number b_0, and the constraint is implemented by introducing a chemical potential λ_0. Therefore, the MF Hamiltonian is written as:

$$H_{mf} = -t\sum_{j=1}^{N-2}\sum_\sigma \left(c_{j\sigma}^\dagger c_{j+1\sigma} + h.c.\right) + \sum_\sigma \tilde{\varepsilon}_d f_\sigma^\dagger f_\sigma$$
$$-\sum_\sigma \left(\tilde{t}_L f_\sigma^\dagger c_{1\sigma} + \tilde{t}_R e^{i\phi} c_{N-1\sigma}^\dagger f_\sigma + h.c.\right) + \lambda_0(b_0^2 - 1), \quad (2)$$

which is essentially a noninteracting system with a set of renormalized parameters $\tilde{\varepsilon}_d = \varepsilon_d + \lambda_0$ and $\tilde{t}_{L(R)} = b_0 t_{L(R)}$. Since the conduction electrons themselves do not form a *complete* set, the Fourier transformation can not be used to diagonalize H_{mf}. As a result, the ground state energy E_{gs} can only be evaluated by exact diagonalization as

$$E_{gs} = \sum_{m\sigma}^{occ} \varepsilon_{m\sigma}(\lambda_0, b_0) + \lambda_0(b_0^2 - 1), \quad (3)$$

where the summation over m includes all occupied levels of H_{mf}. The values of λ_0 and b_0 can be determined self-consistently by minimizing E_{gs} with respect to λ_0 and b_0. Once the solutions λ_0^*, b_0^* and $E_{gs} = E_{gs}^*(\lambda_0^*, b_0^*)$ are obtained, one can calculate the conduction electron DOS at site N_i by

$$\rho_{N_i\sigma}(\omega) = -\frac{1}{\pi}\mathrm{Im}\ \left\langle 0 \left| c_{N_i\sigma}(\omega + i\gamma - H_{mf})^{-1} c_{N_i\sigma}^\dagger \right| 0 \right\rangle,$$

and the PC: $I = -\frac{e}{\hbar}\frac{\partial E_{gs}}{\partial \phi}$, where $|0\rangle$ represents the vacuum state, and γ is introduced to denote the half-maximum width of the spectrum lines in the DOS. Note that the DOS of QD is given by $\rho_{QD}(\omega) = b_0^2 \rho_{0\sigma}(\omega)$, and the "Kondo correlation energy" T_K for the finite-size systems can be defined by the energy gain due to coupling between the QD and the ring:

$$T_K = \varepsilon_d - \varepsilon_F - (E_{gs} - E_{gs}^0), \quad (4)$$

where E_{gs}^0 denotes the ground state energy of the noninteracting Hamiltonian H_0 with electron number N_e and an *open* boundary condition, and ε_F is the energy of the highest occupied level. T_K is thus the Kondo temperature in the finite size system, and it will approach T_K^0 in the thermodynamical limit ($L \to \infty$). In this sense, we will refer to T_K as a *mesoscopic* Kondo temperature.

The Anderson impurity model in QD realizations also exhibits distinct behaviors in different regimes[5]. Here we will mainly focus on the Kondo regime, namely, the highest occupied energy level of the QD has a single occupancy. As a typical case, we choose $\varepsilon_d = -0.7t$, $t_L = t_R = 0.35t$, and $\Gamma = 0.245t$, corresponding to $T_K^0 = 0.0105t$ or $\xi_K^0 = 191$ in the thermodynamic limit.

DOS of QD. — In the absence of the external magnetic flux, the DOS of QD $\rho_{QD}(\omega)$ is obtained by numerically solving the SBMF self-consistent equations for various ξ_K^0/L and are summarized in Fig. 1, where the half maximum width of the spectrum lines has been chosen as $\gamma = 0.5T_K^0$, and different choices of γ will not change the results much. For $\xi_K^0 \ll L$, the shape of the Kondo resonance is indistinguishable from the bulk case. When L is decreased down to ξ_K^0, however, it splits up into a set of subpeaks, in a way which depends strongly on the total numbers of lattice sites N (*modulo* 4). The case of $N = 4n + 2$ shows two main peaks with nearly the same weight around ε_F, whereas the others only have a single main peak at slightly different positions. Despite developing subpeaks, the Kondo resonance retains its basic feature, *i.e.*, the profile of the DOS around ε_F is preserved within a few T_K^0. In other words, the Kondo correlations induced by spin-flip processes between the singly occupied electron on the QD and the conduction electrons persist even in a very small system.

Features for the $\xi_K^0 \sim L$ case are *mainly* determined by the highest occupied and lowest unoccupied single particle energy levels of $\mathcal{H}_{mf}$. For $N = 4n$, when the localized electron on QD binds a delocalized electron at the energy range $|\varepsilon| \lesssim \Gamma$ to form a Kondo singlet near $\epsilon_F = 0$, the energy difference between the highest occupied and lowest unoccupied levels is very small, and a single peak is dominant in the DOS. In contrast, for $N = 4n + 2$, there is a large difference in the resulting highest occupied and lowest unoccupied energy levels, so the Kondo resonance peaks appear both below and above ε_F with almost the same weight. On the other hand, for the odd parity cases of $N = 4n \pm 1$, the highest energy levels are singly occupied below and above ε_F, respectively, and a single Kondo resonance thus appears below and above ε_F separately. This feature may have significant consequences.

The DOS of the QD is also strongly affected by the external magnetic flux. This is illustrated in Fig. 2, which shows the ϕ dependence of $\rho_{QD}(\omega)$ for $\xi_K^0/L = 1.0$. A striking feature is that the DOS *with N sites and zero flux is exactly equal to the one with $N + 2$ sites and a half flux quantum.* Such a feature is related to the nature of the strong coupling fixed point for the model, where one electron is trapped in the symmetric sites around the impurity and other delocalized conduction electrons gain a resonant phase shift from the scattering off the Kondo singlet. It is therefore sufficient to consider only the case of $N = 4n$ and $4n + 1$. For even parity of $N = 4n$, the single main peak in the DOS gradually splits into two symmetric peaks as ϕ increases to π, and they recombine again into a single peak as ϕ is further increased to 2π. For odd parity of $N = 4n + 1$, the situation is quite different. A single main peak in DOS persists asymmetrically in the whole range of ϕ, and its position is shifted with a period of 2π. However, in this odd par-

ity cases there is an important symmetry in the DOS of QD: $\rho_{QD}(-\omega,\phi)=\rho_{QD}(\omega,\pi+\phi)$, leading to the period halving in the PCs.

Kondo screening cloud. — In order to determine the size of the Kondo screening cloud, Fig. 3a illustrates the DOS of the QD and selected lattice sites for a very large ring $\xi_K^0/L=0.1$. At $\omega\approx 0$, the DOS of lattice sites N_i *near* the QD is strongly affected by the Kondo resonance, and clearly exhibits a parity-dependence, *i.e.*, it is enhanced for $N_i=$ even and suppressed for $N_i=$ odd. However, such an influence does weaken significantly once the lattice site is away from the QD. This is illustrated in the change of DOS at ε_F, as shown in Fig. 3b, which is obtained by substracting the background for the noninteracting part H_0. We observe that $\Delta\rho_{N_i\sigma}(\omega=0)$ drops *exponentially* with increasing N_i as expected. The decay length ξ_K deduced from numerical fitting is roughly 190, which is close to the Kondo correlation length scale in the thermodynamic limit $\xi_K^0=191$. Note that this is not an accurate procedure to determine this characteristic length scale.

PC. — The most convenient way to detect the above Kondo screening cloud in experiments is to measure the PC in a ring induced by the magnetic flux. Such measurements have been performed recently on micron size rings not containing a QD[16] and slightly different experimental setup with a QD[7]. In Fig. 4 we show the PC vs magnetic flux for $\xi_K^0/L=0.3$ (dashed line) and 1.5 (solid line). A striking feature can be clearly seen $I^{N+2}(\phi)=I^N(\phi+\pi)$ due to the fact that the structures of DOS of QD have an exact π shift from the system with N sites to that with $N+2$ sites. It is obvious that the behavior of PC differs greatly in the limit $\xi_K^0/L\ll 1$ from that for $\xi_K^0/L\sim 1$. In the former case the system resembles an idea metallic ring, implying a high electron transmission through the QD. When L becomes comparable to ξ_K^0, the PC does weaken systematically and their profiles are close to sinusoidal. Moreover, the PC for odd parity appears to be much smaller than that for even parity, which also indicates a weakening of the Kondo screening effect and the QD simply acts as an *incoherent* scatter. Note that these features are in good agreement with the recent perturbation theory results[14], but are partly in contradiction with those of variational calculations[13].

In order to fully display the dependence on the ring circumference, the PCs and Kondo correlation energies T_K are calculated as functions of ξ_K^0/L in the cases of $\phi=\pi/4$ and $\pi/2$, displayed in Fig.5. We find the PCs interpolate smoothly between the limits of small and large ξ_K^0/L. Both I/I_0 and T_K/T_K^0 curves follows *universal* scaling functions of the ratio ξ_K^0/L, depending on the total number of electrons (*modulo* 4). It is rather surprising that the *mesoscopic Kondo temperatures T_K in small rings are much higher than the bulk value T_K^0*, implying that the corresponding Kondo correlation lengths ξ_K are much *smaller* than the bulk value ξ_K^0.

Finally, we study the properties of the PCs for different occupations of the highest occupied energy level of QD by tuning the dot energy level ε_d. In Fig. 6 the PC is shown as a function of ε_d for various ξ_K^0/L at $\phi=\pi/4$. For different parities, the PCs exhibit an asymmetric structure and their maxima appear near the crossover boundary of the Kondo and mixed-valence regimes. In the Kondo regime, the PCs are *suppressed* as L decreases, indicating the effects of weakening in the Kondo-assisted tunnelings, while in the mixed-valence regime, however, the PCs are almost unchanged as L varies. These distinct features suggest that the tunneling mechanisms in the Kondo and mixed valence regimes are quite different.

In conclusion, we have calculated the mesoscopic Kondo screening effect in a single-electron transistor embedded in a metallic ring. The Kondo resonance is found to be strongly dependent on the dimensionless ratio ξ_K^0/L, the total number of electrons (*modulo* 4), and the external flux threading the ring. The screening effects on the PCs are expected to be observable in experiments.

H. Hu acknowledges the support of Profs. Jia-Lin Zhu and Jia-Jiong Xiong, and a research grant from NSF-China (No. 19974019). G.-M. Zhang was supported by NSF-China (Grant No. 10074036) and the Special Fund for Major State Basic Research Projects of China (G2000067107).

[1] A. C. Hewson, *The Kondo Problem to Heavy Fermions* (Cambridge University Press, Cambridge, 1993).
[2] D. Goldhaber-Gordon *et al.*, Nature **391**, 156 (1998).
[3] S. M. Cronenwett *et al.*, Science **281**, 540 (1998).
[4] F. Simmel *et al.*, Phys. Rev. Lett. **83**, 804 (1999).
[5] D. Goldhaber-Gordon *et al.*, Phys. Rev. Lett. **81**, 5225 (1998).
[6] W. G. van der Wiel *et al.*, Science **289**, 2105 (2000).
[7] R. Schuster *et al.,* Nature **385**, 417 (1997); Y. Ji *et al.*, Science **290**, 779 (2000).
[8] L. I. Glazman and M. E. Raikh, JETP Lett. **47**, 452 (1988).
[9] T. K. Ng and P. A. Lee, Phys. Rev. Lett. **61**, 1768 (1988).
[10] A. A. Zvyagin and I. N. Karnaukhov, Mod. Phys. Lett. B **8**, 937 (1994); A. A. Zvyagin and P. Schlottmann, Phys. Rev. B **54**, 15191 (1996), references therein.
[11] M. Büttiker and C. A. Stafford, Phys. Rev. Lett. **76**, 495 (1996).
[12] V. Ferrari, *et al.*, Phys. Rev. Lett. **82**, 5088 (1999).
[13] K. Kang and S.-C. Shin, Phys. Rev. Lett. **85**, 5619 (2000).
[14] I. Affleck and P. Simon, Phys. Rev. Lett. **86**, 2854 (2001).
[15] W. B. Thimm, J. Kroha, and Jan von Delft, Phys. Rev. Lett. **82**, 2143 (1999).
[16] V. Chandrasekhar, *et al.*, Phys. Rev. Lett. **67**, 3578 (1991); D. Mailly, *et al.*, Phys. Rev. Lett. **70**, 2020 (1993).

Figures Captions

Fig.1. $\rho_{QD}(\omega)$ for various values of ξ_K^0/L in the absence of a magnetic flux. The number of lattice sites

$N = L$ corresponds to (a) $4n$, (b) $4n+1$, (c) $4n+2$ and (d) $4n+3$, respectively. Curves are offset by 1.5 units each, and the half-maximum width of the spectrum lines $\gamma = 0.5T_K^0$.

Fig.2. $\rho_{QD}(\omega)$ of $\xi_K^0/L = 1.0$ for different external flux. In each subplot, from the bottom up, $\phi = 0 \sim 2\pi$ is increased at steps of 0.2π. Curves are offset by 2 units each.

Fig.3. (a) $\rho_{QD}(\omega)$ and selected lattice sites $\rho_{N_i}(\omega)$ for $\xi_K^0/L = 0.1$. The dashed lines denote the corresponding DOS for H_0, and curves labeled by $N_i = 1, 2, 191$, and 192 are offset by $0.1, 0.6, 0.8$, and 1.1 units, respectively. The curve for $\rho_{QD}(\omega)$ is reduced by five times. (b) The change of DOS $\Delta\rho_{N_i\sigma}(\omega = 0)$ is calculated by substracting the background for H_0 as a function of the lattice site N_i . The solid line fits the exponential decay and a characteristic length is obtained $\xi_K \sim 190$.

Fig.4. Persistent currents versus flux with the total number of lattice sites $4n+i$ ($i = 0, 1, 2, 3$) for $\xi_K^0/L = 0.3$ (dashed lines) and for $\xi_K^0/L = 1.5$ (solid lines). I_0 denotes the corresponding PC of an ideal metallic ring.

Fig.5. Persistent currents and Kondo temperature T_K as functions of ξ_K^0/L for $\phi = \pi/4$ and $\pi/2$. Both I/I_0 and T_K/T_K^0 curves follow universal scaling functions of the ratio ξ_K^0/L.

Fig.6. Occupation number of the highest occupied energy level of QD (solid lines) n_d and PCs I/I_0. The dashed, dotted, dash-dotted, and dash-dot-dotted lines show the data for $\xi_K^0/L = 0.3$, 0.6, 1.2, and 2.4, respectively, as functions of ε_d for different parities at $\phi = \pi/4$.

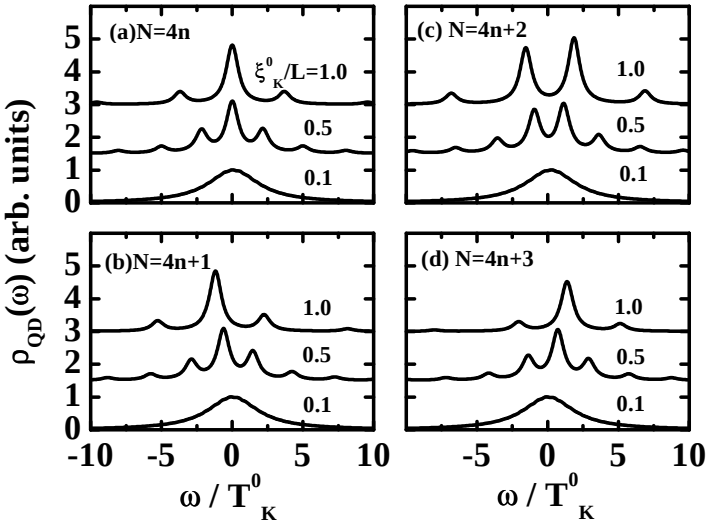
(a)N=4n
(c) N=4n+2
(b)N=4n+1
(d) N=4n+3
ξ⁰K/L=1.0
1.0
0.5
0.1
ρQD(ω) (arb. units)
ω / T⁰K
-10
-5
0
5
10

Fig. 1

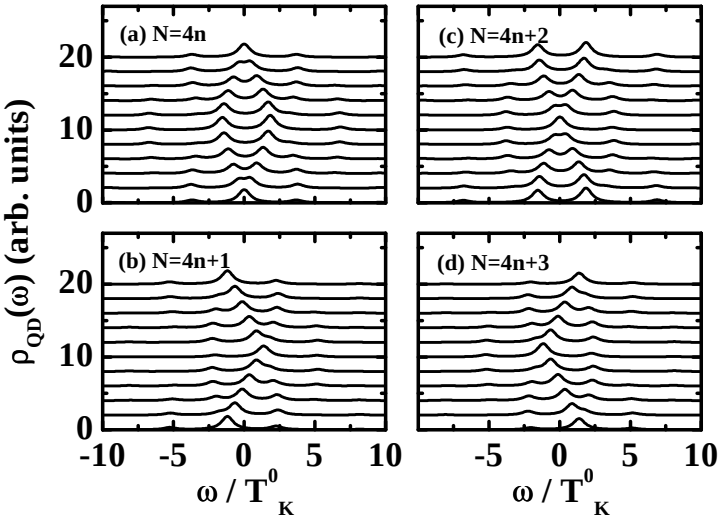
(a) N=4n
(c) N=4n+2
(b) N=4n+1
(d) N=4n+3
20
10
0
-10
-5
0
5
10
$\rho_{QD}(\omega)$ (arb. units)
ω / T^0_K

Fig. 2

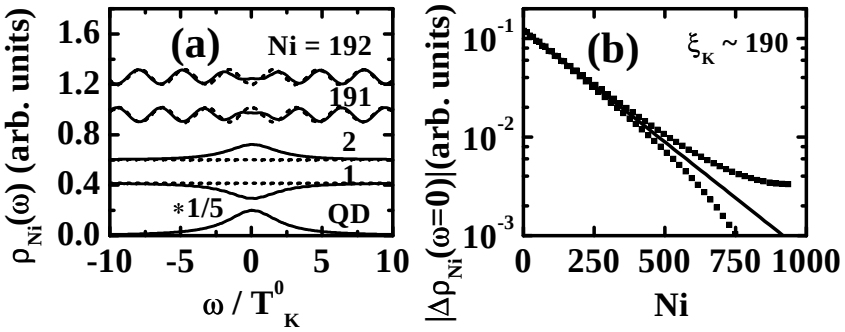
(a)
Ni = 192
191
2
1
*1/5
QD
1.6
1.2
0.8
0.4
0.0
-10
-5
0
5
10
ω / T⁰K
ρNi(ω) (arb. units)
(b)
ξK ~ 190
10-1
10-2
10-3
0
250
500
750
1000
Ni
|ΔρNi(ω=0)|(arb. units)

Fig. 3

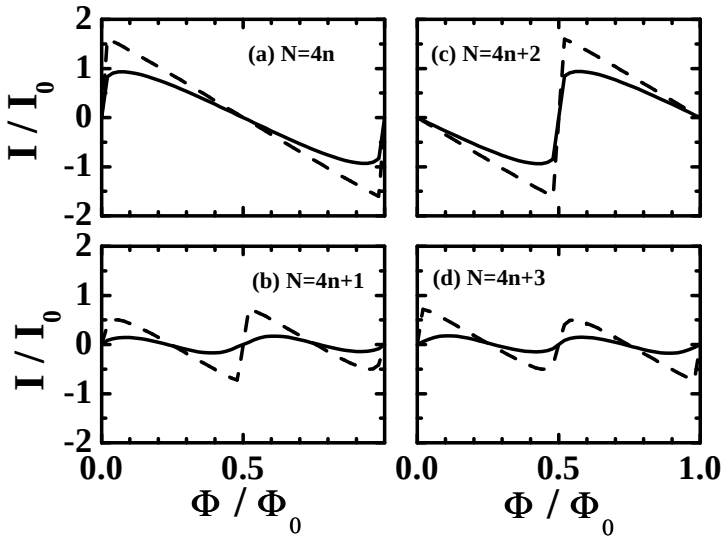

Fig. 4

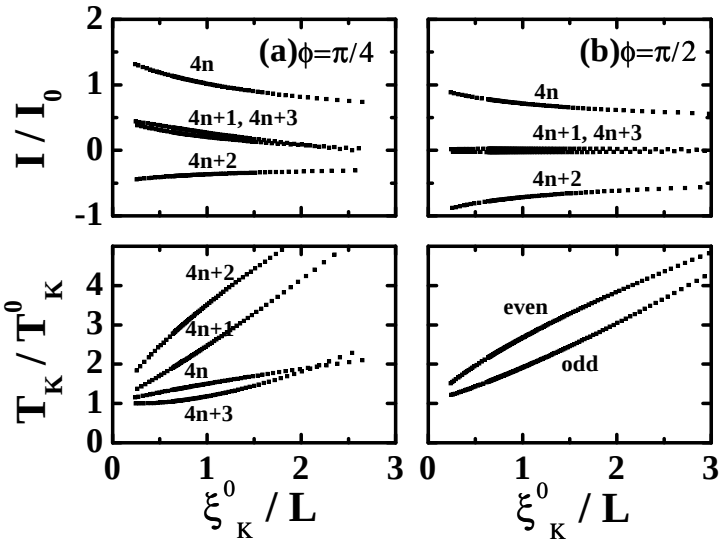

Fig. 5

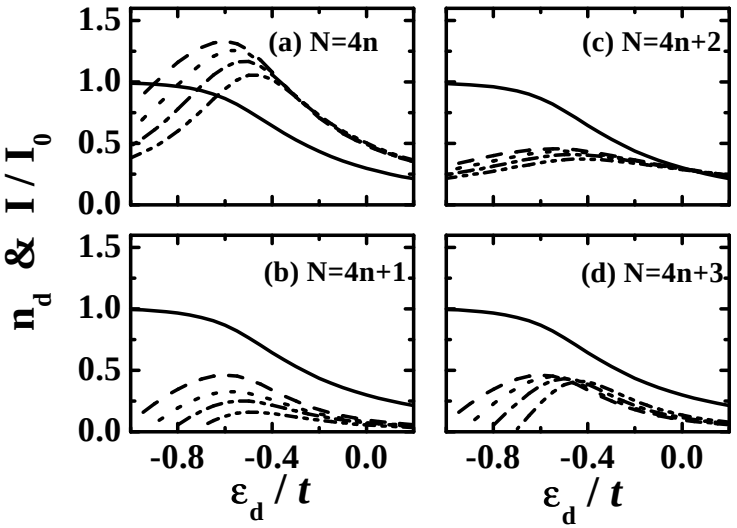
(a) N=4n
(c) N=4n+2
(b) N=4n+1
(d) N=4n+3
1.5
1.0
0.5
0.0
-0.8
-0.4
0.0
n_d & I / I_0
ε_d / t

Fig. 6